PHILOSOPHICAL TRANSACTIONS OF THE ROYAL SOCIETY A

Phil. Trans. R. Soc. A (2007) **365**, 699–714
doi:10.1098/rsta.2006.1939
Published online 16 January 2007

Turbulent flow in smooth and rough pipes

By J. J. Allen[1], M. A. Shockling[2], G. J. Kunkel[3] and A. J. Smits[3,*]

[1]*Department of Mechanical Engineering, New Mexico State University, Las Cruces, NM 88003, USA*
[2]*GE Global Research, 1 Research Circle, Niskayuna, NY 12309, USA*
[3]*Department of Mechanical and Aerospace Engineering, Princeton University, Princeton, NJ 08540, USA*

Recent experiments at Princeton University have revealed aspects of smooth pipe flow behaviour that suggest a more complex scaling than previously noted. In particular, the pressure gradient results yield a new friction factor relationship for smooth pipes, and the velocity profiles indicate the presence of a power-law region near the wall and, for Reynolds numbers greater than about 400×10^3 ($R^+>9\times10^3$), a logarithmic region further out. New experiments on a rough pipe with a honed surface finish with $k_{\rm rms}/D=19.4\times10^{-6}$, over a Reynolds number range of 57×10^3–21×10^6, show that in the transitionally rough regime this surface follows an inflectional friction factor relationship rather than the monotonic relationship given in the Moody diagram. Outer-layer scaling of the mean velocity data and streamwise turbulence intensities for the rough pipe show excellent collapse and provide strong support for Townsend's outer-layer similarity hypothesis for rough-walled flows. The streamwise rough-wall spectra also agree well with the corresponding smooth-wall data. The pipe exhibited smooth behaviour for $k_{\rm s}^+\leq3.5$, which supports the suggestion that the original smooth pipe was indeed hydraulically smooth for $Re_D\leq24\times10^6$. The relationship between the velocity shift, $\Delta U/u_\tau$, and the roughness Reynolds number, $k_{\rm s}^+$, has been used to generalize the form of the transition from smooth to fully rough flow for an arbitrary relative roughness $k_{\rm rms}/D$. These predictions apply for honed pipes when the separation of pipe diameter to roughness height is large, and they differ significantly from the traditional Moody curves.

Keywords: pipe flow; turbulence; roughness; Reynolds number

1. Introduction

The law of the wall is a description of the mean velocity profile in wall-bounded flows and has been accepted as one of the most important concepts in the turbulence community for at least 70 years. Barenblatt *et al.* (1997) and Barenblatt & Chorin (1998) however proposed that the velocity profile is not universal but in fact a weakly varying power law with coefficients that vary with the Reynolds number. This suggestion has important implications for the prediction of high Reynolds number flows because the correct formulation of scaling laws enables us to make

* Author for correspondence (asmits@princeton.edu).

One contribution of 14 to a Theme Issue 'Scaling and structure in high Reynolds number wall-bounded flows'.

predictions beyond the range of Reynolds numbers achievable in the laboratory. For example, according to the specification listed on EuRoPol GAZ's website, the Yamal–Europe pipeline operates at Reynolds numbers greater than 50×10^6. With a volume flow rate of 32.3×10^9 m^3 of gas per year, accurate drag prediction is of the utmost importance.

Running counter to the power-law claims are the results of Zagarola & Smits (1998), and more recently by McKeon *et al.* (2004*a*), who found strong experimental evidence for the existence of the law of the wall in pipe flow over three orders of magnitude in Reynolds number, supporting the arguments made earlier by George & Castillo (1997). More precisely, the results indicate the presence of a power-law region near the wall and, for Reynolds numbers greater than 400×10^3 ($R^+>9\times10^3$), a logarithmic region further out. Here, $R^+=Ru_\tau/\nu$, where $u_\tau=\sqrt{\tau_w/\rho}$ is the friction velocity, R is the pipe radius ($=D/2$) and ν is the kinematic viscosity. In other words, in inner-layer variables,

$$\frac{U}{u_\tau}=\frac{1}{\kappa}\ln\frac{yu_\tau}{\nu}+B,$$

or

$$U^+=\frac{1}{\kappa}\ln y^+ + B, \tag{1.1}$$

where U is the mean velocity and $U^+=U/u_\tau$. In outer-layer variables,

$$U^+_{CL}-U^+=\frac{1}{\kappa}\ln\frac{y}{R}+B', \tag{1.2}$$

where U_{CL} is the centreline velocity. The log law was found for $600<y^+<0.12R^+$, and the von Kármán constant κ, the additive constant B for the log law using inner-layer scaling and the additive constant B' for the log law using outer-layer scaling were found to be 0.421 ± 0.002, 5.60 ± 0.08 and 1.20 ± 0.10, respectively. These data were obtained in the Princeton/ONR Superpipe, which uses compressed air up to 20 MPa in a 129 mm diameter pipe to achieve the Reynolds numbers Re_D up to 35×10^6. Here, $\mathrm{Re}_D=D\bar{U}/\nu$, where $\overline{U}$ is the velocity averaged over the pipe cross-section.

These experimental datasets however have not led to a full resolution of the controversy in relation to the nature of the mean profile since there is a continuing debate on the effects of surface roughness. Although it is intuitive that flow over a rough surface will experience a larger drag than a smooth surface, it is not completely clear when and how a rough surface begins to affect the mean velocity profile, much less the higher order moments and turbulence structure. As the Reynolds number increases, a point is reached where the size of the smallest eddies in the flow is comparable to the size of the roughness elements k, and viscous effects are no longer sufficient to damp the effects of the perturbation. Beyond this transitional regime, a point is reached at higher Reynolds numbers where the flow becomes fully rough, and further increases in Reynolds number no longer have an effect on the friction factor. In the fully rough regime, the wall shear stress varies quadratically with the velocity, implying that form drag on the roughness elements is the principal source of the axial pressure drop. All flows eventually become rough as the Reynolds number increases and the relative size of the smallest scales in the flow decreases.

Whether roughness becomes relevant above a specific Reynolds number, or whether it is always present and just difficult to detect, has been raised in a recent paper by Bradshaw (2000).

Experimentally, the symptoms of roughness in pipe flows can be detected by a number of means. First, there is a departure of the friction factor–Reynolds number relationship above that for hydraulically smooth turbulent pipe flow. Second, there is a downward shift in the logarithmic layer (equivalently, a decrease in the additive constant in the log law). In the outer region of the flow, however, it is expected that roughness manifests itself only in terms of a changing wall stress, so that the mean velocity and the turbulence intensity profiles in outer-layer variables are unaffected by roughness, assuming, of course, that k remains small compared with D. This is known as Townsend's hypothesis of outer-layer similarity (Townsend 1976).

The recent work of Perry *et al.* (2001) raised the possibility of roughness being present in the data of Zagarola & Smits (1998) for Reynolds numbers greater than 400×10^3. This conclusion was based principally on (i) the use of the MacMillan (1956) Pitot probe corrections, (ii) the observation that the datasets of Zagarola & Smits (1998) appeared to be departing from Prandtl's 'universal' friction relationship (Schlichting 1979) and began following Colebrook's transitional roughness function (Colebrook 1939), and (iii) the presence of a small downward shift in the velocity profiles at high Reynolds numbers (called 'steps'). Although these issues were comprehensively resolved by McKeon *et al.* (2004*a*), the work of Perry *et al.* (2001) draws into the spotlight the use and the validity of the Colebrook functions to describe transitional flows.

Historically, the behaviour of an arbitrary surface in the fully rough regime has been related to an 'equivalent sand-grain roughness value' from the work of Nikuradse (1933). Nikuradse conducted experiments with a series of pipes, each of which was coated with sand with a narrow size distribution. Nikuradse's data in the transitionally rough regime show the friction factor gradually increasing above the smooth curve, reaching a minimum value, before rising and levelling off to the fully rough value. We call this behaviour 'inflectional'. Almost all the subsequent rough-wall studies compare the value of the friction factor in the fully rough regime with Nikuradse's values and hence assign an equivalent sand-grain roughness to the surface under consideration. The transitional behaviour for a particular surface depends critically on the geometric nature of the roughness and hence any discussion regarding the onset of rough-wall behaviour needs to consider this particular aspect. In an attempt to classify the data available at the time, Colebrook (1939) developed a curve fit to describe transitional roughness, which is expressed as

$$\frac{1}{\sqrt{\lambda}} = 1.74 - 2\log\left(\frac{k_s}{R} + \frac{18.6}{Re_D\sqrt{\lambda}}\right), \tag{1.3}$$

where k_s is the equivalent Nikuradse sand-grain roughness value for the surface and λ is the friction factor, defined by

$$\lambda = \frac{-\frac{\mathrm{d}p}{\mathrm{d}x}D}{\frac{1}{2}\rho\bar{U}^2},$$

where $\mathrm{d}p/\mathrm{d}x$ represents the pressure gradient in the pipe. Equation (1.3) describes a monotonic change in the friction factor from smooth to fully rough, in that the fully rough value is approached from above, and held by Colebrook to be

representative of 'natural or commercial surface finishes'. It is also the basis for the widely used Moody diagram (Moody 1944). A key element of the argument given by Perry *et al.* (2001) is that the data of Zagarola & Smits (1998) follow a Colebrook-type curve for the stated value of $k_s = 3k_{rms} = 0.45$ μm. In order to verify this assumption, experiments were performed to determine the nature of the transitionally rough regime for a surface of similar geometric distribution to that used in the experiments of Zagarola & Smits (1998) and McKeon *et al.* (2004*a*). The results are described in detail by Shockling (2005) and Shockling *et al.* (2006).

2. Experiments and results

The experiments were performed in the Princeton University Superpipe facility, capable of generating Reynolds numbers from 31×10^3 to 35×10^6 (figure 1). Details of the operation of this unique high-pressure facility can be found in Zagarola (1996) and Zagarola & Smits (1998).

(*a*) *Smooth pipe*

We use as a basis for comparison the smooth pipe results presented by McKeon *et al.* (2004*a*,*b*) and Morrison *et al.* (2002, 2004). Figure 2*a* shows the friction factor data for the smooth pipe compared to the Blasius and Prandtl correlations. The Blasius relation is valid for a Reynolds number up to 10^5. Prandtl's 'universal' correlation is given by

$$\frac{1}{\sqrt{\lambda}} = 2.0 \log\left(Re_D\sqrt{\lambda}\right) - 0.8. \tag{2.1}$$

The constants suggested by Prandtl were found by curve fitting the smooth-wall pipe data of Nikuradse (1932) over the Reynolds number range $3.1\times10^3 < Re_D < 3.2\times10^6$. For Reynolds numbers greater than about 10^6, the Superpipe data lie above this line, and McKeon *et al.* (2005) proposed a new correlation for smooth pipe flow, given by

$$\frac{1}{\sqrt{\lambda}} = 1.930 \log\left(Re_D\sqrt{\lambda}\right) - 0.537, \tag{2.2}$$

which fit their data for $31\times10^3 \leq Re_D \leq 35\times10^6$ to within 1.25%.

The mean velocity profiles for the smooth pipe are shown in figure 2*b*. The profiles were obtained using a Pitot probe in combination with a wall static pressure tapping and are subject to corrections for the effects of Reynolds number, wall proximity and velocity gradient. The original dataset presented by Zagarola & Smits (1998) was based on an inadequate understanding of the Reynolds number effects on the static pressure reading, and as a result showed a systematic decrease in the additive constant in the logarithmic law (steps), which can be interpreted as the onset of roughness. However, McKeon & Smits (2002) determined the corrections appropriate to high Reynolds number, and demonstrated that when these corrections were applied to the data the steps became negligible, concluding that the surface was smooth for $Re_D \leq 18\times10^6$ (at least). Nevertheless, the higher friction factors observed at higher Reynolds numbers still suggest the influence of roughness.

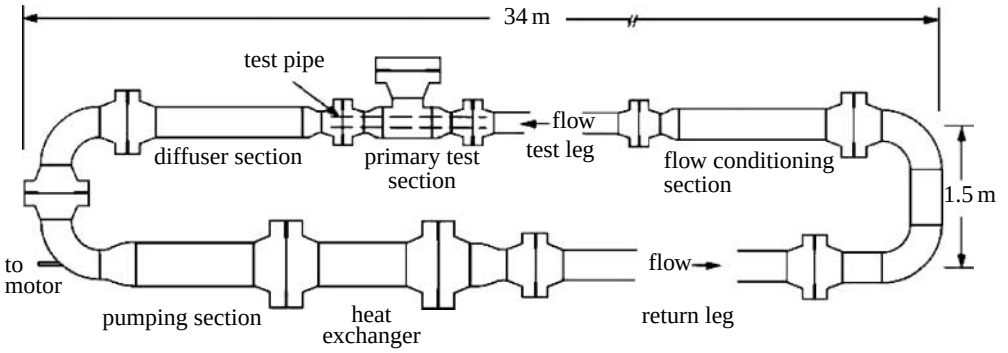

Figure 1. Superpipe apparatus.

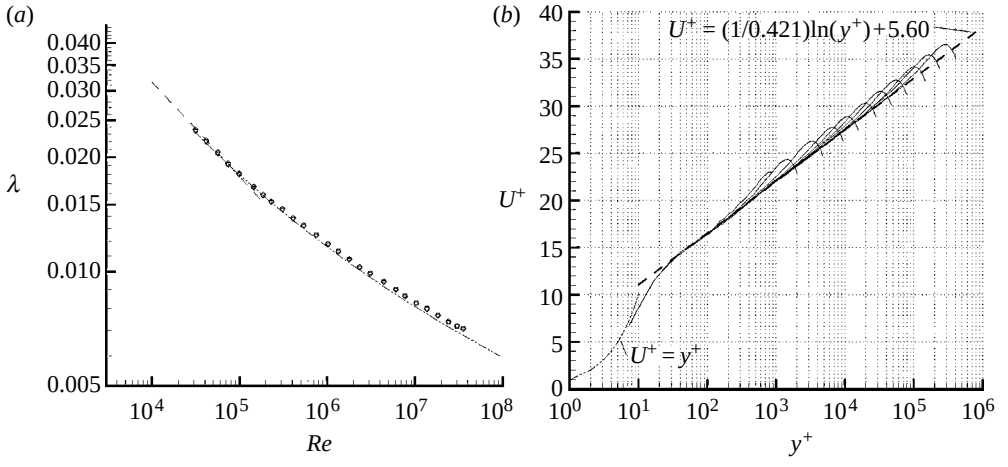

Figure 2. (*a*) Smooth-wall friction factor data compared with the Blasius (dashed line) and Prandtl friction factor relationships (dashed–dotted line). (*b*) Smooth-wall mean velocity profiles for every second Reynolds number, starting from $Re_D = 31 \times 10^6$ to $Re_D = 18 \times 10^6$. Figures from McKeon *et al.* (2004*a*).

(*b*) *Rough pipe*

The difficulty in making conclusive statements regarding the characteristics of the original Superpipe surface is that little is known on the behaviour of surfaces with extremely small values of k/D and, more particularly, on the behaviour of flow in pipes with honed surface finishes. For the smooth pipe flow experiments, $k_{\mathrm{rms}}/D = 1.16 \times 10^{-6}$ (determined independently using comparator plates, surface stylus measurements and optical imaging of the surface). This is a very small value, and one where little previous knowledge exists, and so an experiment was performed to study these flows in detail (see Shockling (2005) and Shockling *et al.* (2006) for further details). Given the capabilities of the Superpipe facility, it is possible, in a single apparatus, to study the effects of roughness from the hydraulically smooth regime to the fully rough regime. Of particular interest here is the transitional roughness behaviour at small values of the roughness parameter k/D.

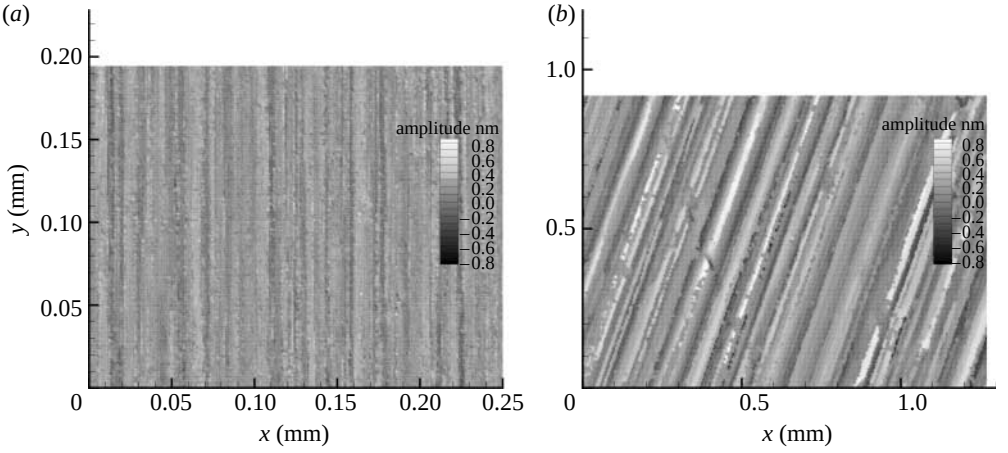

Figure 3. Two-dimensional surface plots. (*a*) Original 'smooth' surface studied by Zagarola & Smits (1998) and (*b*) surface of rough pipe studied by Shockling *et al.* (2006).

Developing transitional roughness relationships for a surface finish of the type used by Zagarola & Smits (1998) requires accurate knowledge of the original surface geometry. Non-interfering optical measurements were therefore made of the surface, and a typical image of the original Superpipe surface is shown in figure 3*a*. The mean amplitude of the Superpipe roughness was 0.15 μm (6 μin.), with a characteristic wavelength of order 0.01 mm. The presence of this characteristic wavelength is thought to be a consequence of the honing process used to produce the pipes. To examine the nature of the transition for this surface, a geometrically similar surface with a larger physical scale was needed. A new pipe was fabricated, with a diameter of 128 mm, for installation in the Princeton Superpipe high-pressure facility. An optical image of the new 'rough' surface is shown in figure 3*b*. The mean roughness height of this new surface is 2.5 μm with an associated wavelength of order 0.09 mm. The characteristic grooves imparted by the honing tool in figure 3*b* are inclined relative to the vertical, when compared to figure 3*a*. This is due to the requirement of moving the honing tool at a more rapid speed through the pipe in the rough-wall case. The selection of this surface roughness was predicated on the honing tools available, but it represents a reasonable scaling of both the wavelength and the amplitude of the original Superpipe surface.

The data reported here consist of measurements of the friction factor, mean velocity profile, streamwise turbulence intensity profile and one-dimensional spectrum in a honed pipe with $k_{\mathrm{rms}}/D = 19.4\times10^{-6}$ (about 17 times larger than the original smooth Superpipe surface), over a range of Reynolds numbers from 57×10^3 to 21.2×10^6, where k_{s}^+ varies from 0.17 to 44.4 (k_{s} is the equivalent sand-grain roughness). All the measurements were made at a location 191D downstream from the inlet contraction.

Figure 4 shows the friction factor behaviour over the full range of Reynolds number. The friction factor was determined by evaluating the pressure gradient along the pipe from a series of static pressure port measurements that commenced at 163D downstream from the contraction, at 0.3D intervals to 191D. Error bars have only been shown on λ and not on Re_D, which shows negligible error on a semi-logarithmic plot. The data agree well with the smooth curve relationship of

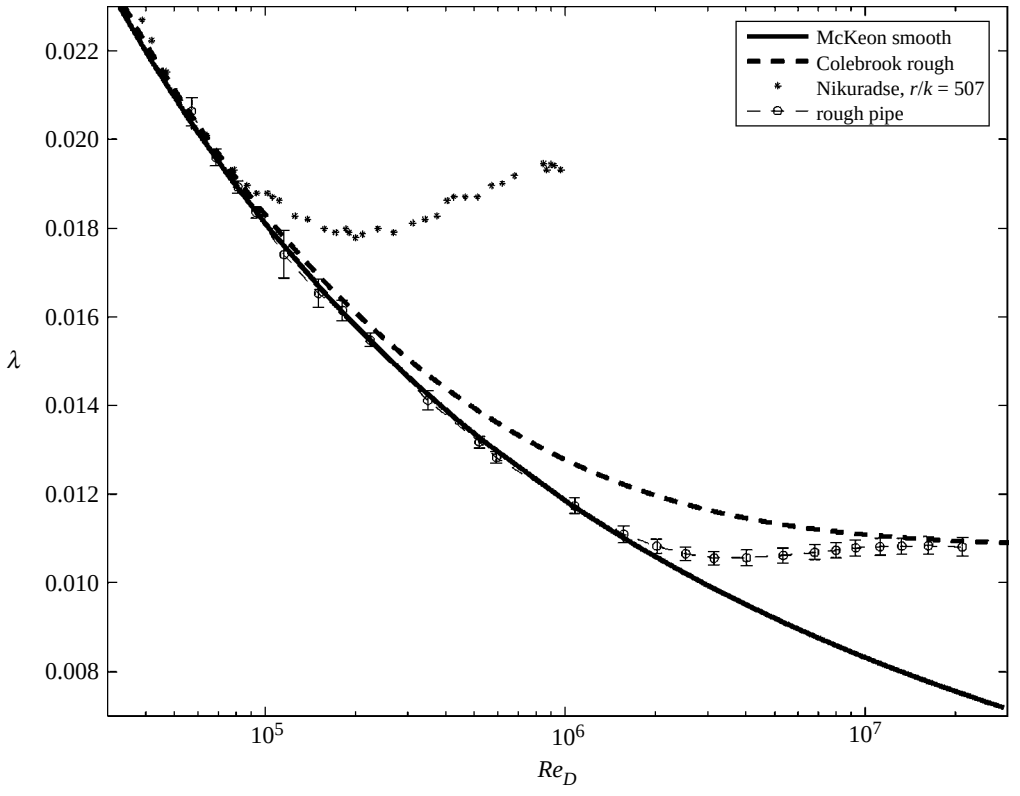

Figure 4. Friction factor λ for the present surface, compared with the rough-wall relations of Colebrook (1939) for the same k_s, the smooth-wall relation of McKeon *et al.* (2005) (equation (2.2)) and the results for the smallest sand-grain roughness used by Nikuradse (1933). Figure from Shockling *et al.* (2006).

McKeon *et al.* (2004*b*) (equation (2.2)) up to $Re_D < 1.6\times10^6$, where the friction factor begins to depart from the smooth curve, reaching a local minimum of $\lambda \simeq 0.0106$ in the region $3.1\times10^6 < Re_D < 4.0\times10^6$. The friction factor then rises to a constant value of $\lambda \simeq 0.0108$ for $Re_D > 10\times10^6$. The equivalent sand-grain roughness for this surface, defined by the friction factor in the fully rough regime, is $k_s = 7.4$ μm, which is in good agreement with the estimate of Zagarola & Smits (1998) of $k_s \simeq 3.0k_{rms}$ for the smooth pipe data.

The Colebrook curve corresponding to $k_s = 7.5$ μm is also shown in figure 4. Clearly, the monotonic Colebrook curve makes a poor prediction for the transitionally rough behaviour of this surface. At the point of departure from the smooth regime, at $Re_D \simeq 1.5\times10^6$, the Colebrook relation overestimates the friction factor by approximately 10%. In the transitional regime, instead of following the Colebrook correlation, the data display an inflectional roughness, similar to the behaviour of the sand-grain roughness tested by Nikuradse (1933), despite the fact that honed surfaces are often classified as, in Colebrook's terms, 'natural' or 'commercial' roughness.

A more sensitive indicator for the effects of roughness is the behaviour of the velocity profiles (figure 5). For $y^+ \geq 600$, corresponding to $Re_D \geq 2.3\times10^5$, the profiles demonstrate the presence of a logarithmic region, which is in agreement with the earlier results of the smooth pipe.

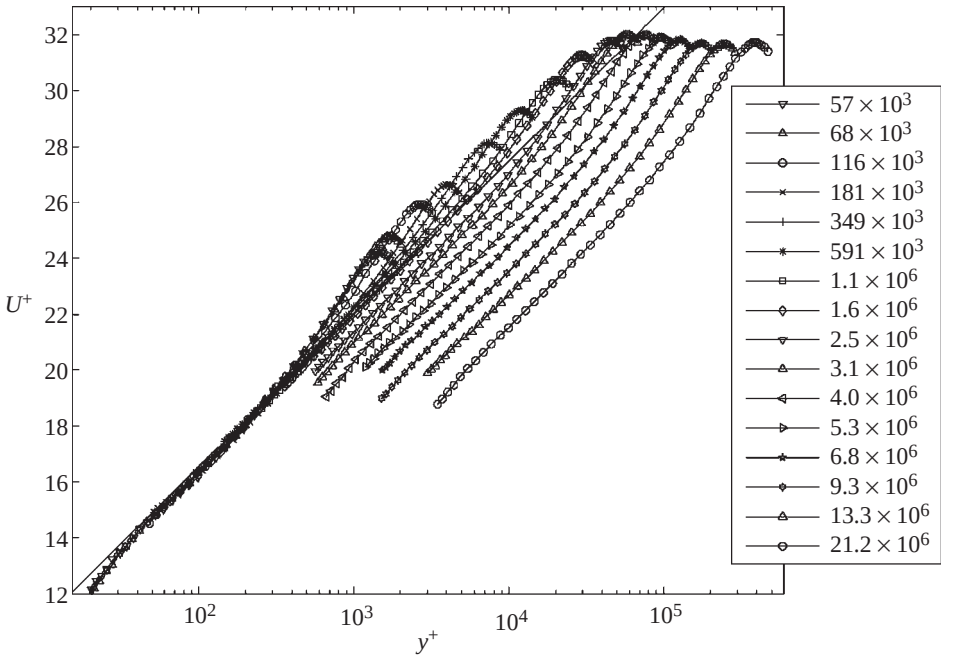

Figure 5. Velocity profiles over the full Reynolds number range. Figure from Shockling *et al.* (2006).

The downward shift of the velocity profile due to roughness can be characterized by the Hama roughness function ΔU^+, defined by writing the logarithmic law for a rough surface as

$$U^+ = \frac{1}{\kappa} \ln y^+ + B - \Delta U^+. \tag{2.3}$$

Here, ΔU^+ was determined by finding the best fit of the data to the log law, with the assumption that $\kappa = 0.421$ and $B = 5.6$ (McKeon *et al.* 2004*a*). The value of 0.421 came from the curve fit to equation (2.1). The behaviour of the Hama roughness function is shown in figure 6*a* as a function of k_s^+. An alternative way of writing equation (2.3) is to use the roughness height as the variable to non-dimensionalize space. Hence,

$$U^+ = \frac{1}{\kappa} \ln \frac{y}{k_s} + B^*. \tag{2.4}$$

As seen from figure 6*b*, the data in the transitional region for B^* follow a curve that resembles more closely the inflectional roughness of Nikuradse (1933) than the monotonic roughness of Colebrook (1939), although the inflectional behaviour does not appear as pronounced as Nikuradse's sand-grain roughness.

Perry *et al.* (2001) claimed that the roughness effects were evident in the smooth Superpipe at values of k_s^+ as low as 0.05. This conclusion was based principally on the assumption that honed surface roughness displays a Colebrook-type transitional behaviour. The data presented here show that honed surface roughness does not deviate from hydraulically smooth conditions until $k_s^+ \simeq 3.5$. The precise value of k_s for the original Superpipe experiment is unknown, since the fully rough condition was not attained in that experiment. Nevertheless, an estimate can be made of the point of departure from smooth

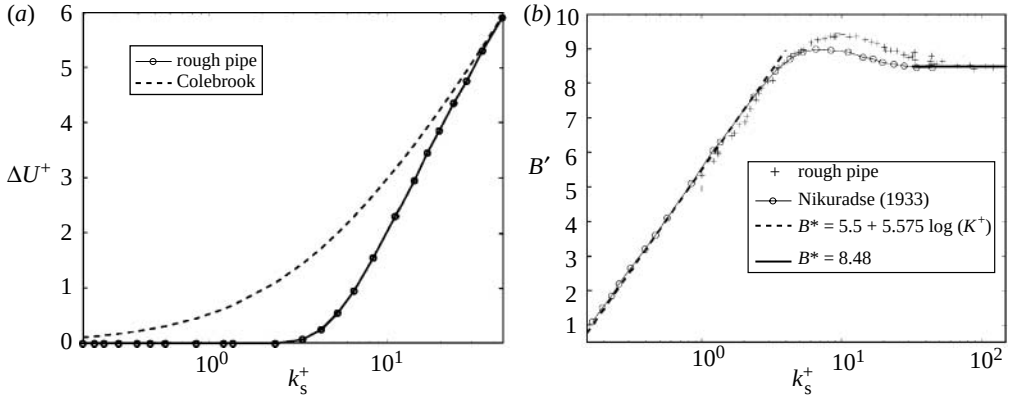

Figure 6. (*a*) Hama roughness function. Dashed line, Colebrook roughness function, with $k_s = 7.4 \times 10^{-6}$ m; straight line, ΔU^+ determined using the constants of McKeon *et al.* (2004*a*). (*b*) Nikuradse roughness function. Figures from Shockling *et al.* (2006).

conditions by assuming that $k_s \simeq 3.0 k_{rms}$ and using a critical k_s^+ of 3.5 as found here for a geometrically similar surface. We find that the original Superpipe should demonstrate hydraulically smooth behaviour up to $Re_D \leq 27 \times 10^6$. The original work by Zagarola & Smits (1998) suggested that the pipe was smooth up to the Reynolds numbers of 24×10^6, in good agreement with the prediction made on the basis of the present work.

Figure 7 shows a collection of velocity profiles for $Re_D \geq 3.5 \times 10^6$ scaled with outer flow variables, y/R. It appears that profiles for the velocity defect, $(U_{cl} - U)/u_\tau$, collapse well, as expected according to Townsend's outer flow similarity hypothesis for rough-wall flows. The collapse in outer-layer variables is comparable to that demonstrated by Zagarola & Smits (1998) for the smooth Superpipe data and by Flack *et al.* (2005) in their rough-wall boundary layer studies.

To further study the effects of roughness in the outer region of the flow and the validity of Townsend's outer flow similarity hypothesis, the rough pipe streamwise turbulence intensity profiles and one-dimensional velocity spectra are compared to similar results from the smooth pipe flow studied by Morrison *et al.* (2004). The instantaneous data were acquired using standard hot-wire anemometry practices with a 2.5 μm platinum/rhodium wire with a length-to-diameter ratio of 160. The wires were operated with an AA Labs anemometer at an over-heat ratio of 1.7. Further details of the hot-wire experiment can be found in Kunkel & Smits (2006). Figure 8 shows the rough pipe turbulence intensities with outer- and inner-layer scaling compared with the corresponding smooth pipe results. The two Reynolds numbers correspond to hydrodynamically smooth-wall ($k_s^+ = 2.1$) and transitionally rough-wall ($k_s^+ = 11$) conditions for the rough pipe. The transitionally rough-wall turbulence intensities agree very well with the results from the smooth pipe flow in the outer region of the flow (outer logarithmic and wake region). As the wall is approached, however, the transitionally rough-wall data begin to deviate and fall below the smooth pipe data. As Kunkel & Smits (2006) explain, this deviation is most likely due to the difficulties of conducting high-Reynolds number hot-wire measurements close to

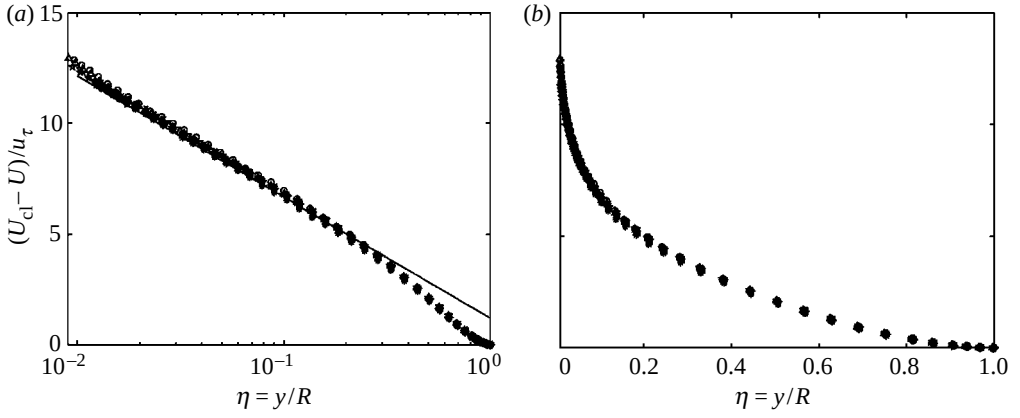

Figure 7. Outer-layer scaling for $349\times10^3 \le Re_D \le 21.2\times10^6$. (*a*) Semi-logarithmic scaling. Solid line, $(U_{cl}-U)/u_\tau = -(1/0.421)\ln(y/R)+1.20$. (*b*) Linear scaling. Figures from Shockling *et al.* (2006).

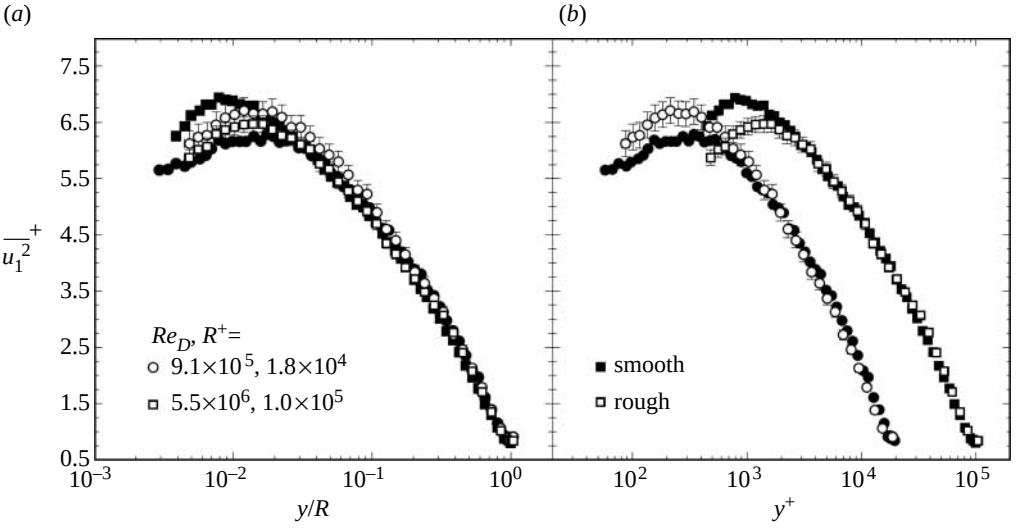

Figure 8. Streamwise turbulence intensities. Hollow symbols, rough pipe data; solid symbols, smooth pipe data (reproduced from Morrison *et al.* 2004). (*a*) Outer-layer scaling and (*b*) inner-layer scaling.

a wall. For the two Reynolds numbers shown, $l^+ = 100$ and 580, and $l/\eta = 27$ and 100, respectively. Here, l is the wire length and η is the Kolmogorov length-scale, which was calculated assuming local equilibrium in the middle of the mean velocity logarithmic region. For comparison, Ligrani & Bradshaw (1987) suggest that $l^+ < 20$–25 for the measured near-wall turbulence level measurement to be affected less than 4%. Our wire lengths are much larger and this will obviously inhibit near-wall measurements. The precise location where the results are free from resolution effects is not known, but it is assumed that this effect is negligible in the outer logarithmic and wake regions of the flow. Aside from the near-wall issues, the data in the outer region are in agreement with Townsend's outer flow

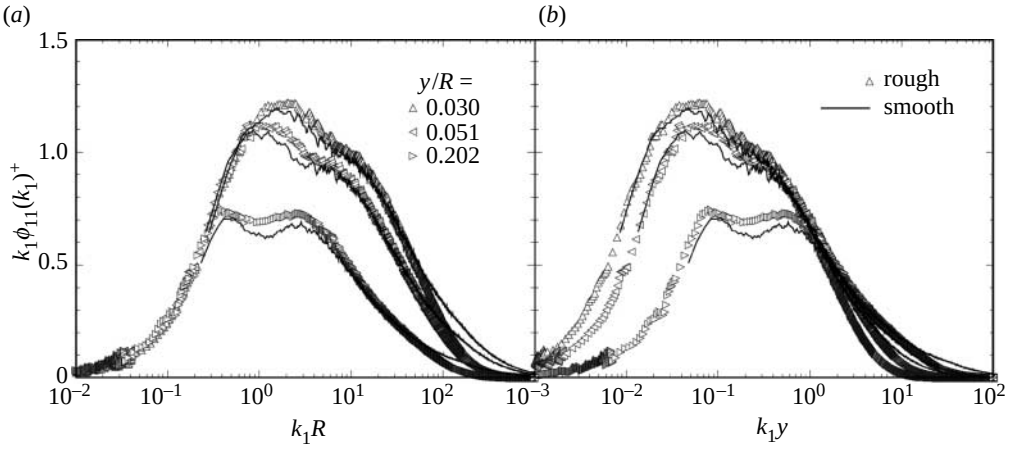

Figure 9. Rough and smooth pipe streamwise velocity spectra at Re_D, $R^+ = 5.7\times10^6$, 1.0×10^5. Hollow symbols, rough pipe data; solid lines, smooth pipe data (reproduced from Morrison *et al.* 2004). (*a*) Outer-layer scaling and (*b*) inner-layer scaling.

similarity hypothesis and the findings of Flack *et al.* (2005); namely, the rough wall does not appear to affect the turbulence intensities in the outer part of the flow (i.e. it simply sets the value of the wall shear stress).

The streamwise velocity spectra are also analysed to investigate any possible structural changes in the flow. Figure 9 shows the comparison of the rough and smooth pipe premultiplied spectra with outer- and inner-layer scaling for the hydrodynamically transitionally rough flow; the agreement is reasonably good. In particular, the energy-containing region of the rough pipe flow is not shifted towards higher wave-numbers, as was found in Krogstad & Antonia (1999). At higher non-dimensional wave-numbers, however, the rough pipe spectra deviate slightly from the smooth pipe spectra. Again, this is thought to be caused by measurement difficulties, especially the physical size of the wire. Kunkel & Smits (2006) found that the attenuation of the spectra at high wave-numbers follows the physical size of the probe (i.e. the larger probe attenuates more high wave-number energy). Also note that the actual energy contribution from the high wave-number region where the attenuation occurs is less than 5% of the total energy (i.e. turbulence intensity) for all datasets, and the overall differences between the smooth and the rough pipe data are less than 2%, which is the measurement accuracy of the turbulence intensities. Therefore, the spectra also appear to support the notion that there is no change in the structure of the flow due to the wall roughness.

3. Generalization of rough pipe results

The rough pipe results bring into the question the validity of the Moody diagram to describe the transitional process in honed pipes with small values of relative roughness. Here, we describe a process that generalizes the rough pipe results to a surface with similar roughness geometry for arbitrary values of relative roughness. This technique assumes a universal wake function, a logarithmic overlap region and a power fit in the viscous and the buffer layers. Full details of the technique are described by Allen *et al.* (2005).

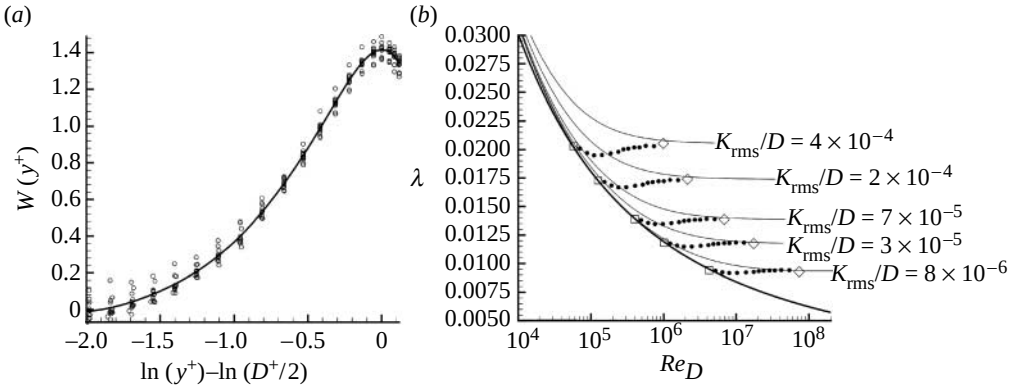

Figure 10. (*a*) Rough pipe universal wake function and (*b*) universal resistance diagram for honed pipes of small relative roughness from Allen *et al.* (2005).

The measurements of Shockling *et al.* (2006) were obtained at one value of relative roughness $c_1 = k_{\mathrm{rms}}/D$. Generation of the friction factor curve for other values of c_1 for a honed surface requires a general expression for the mean velocity profile which can be integrated over the pipe area. The point of departure from the smooth friction factor curve occurs at $k_{\mathrm{s}}^+ \simeq 3.5$. Based on a given c_1 and using $k_{\mathrm{s}} = 3k_{\mathrm{rms}}$, we obtain $u_\tau = 1.167\nu/(Dc_1)$. Substitution into the smooth pipe friction factor relationship (equation (2.2)) results in an expression for the Reynolds number at which the data will depart the smooth curve for a prescribed surface roughness, $Re_{DS} = (6.37/c_1)\ln(3.3/c_1) - 1.77/c_1$. For a given relative roughness c_1 with $k_{\mathrm{s}} = 3k_{\mathrm{rms}}$, the Nikuradse fully rough correlation $1/\sqrt{\lambda} = 2\ln(0.5D/k_{\mathrm{s}}) + 1.74$ can be used to generate the fully rough λ for a prescribed surface roughness, which is expressed as $1/\sqrt{\lambda} = 2\ln(0.167/c_1) + 1.74$. Data from Shockling *et al.* (2006) show that the honed pipe flow is fully rough at $k_{\mathrm{s}}^+ \simeq 60$, so that $u_\tau = 20\nu/(Dc_1)$. Substituting into the relationship for the fully rough friction factor gives $Re_{D\mathrm{R}} = (113.14/c_1)\ln(0.167/c_1) + 98.42/c_1$, where $Re_{D\mathrm{R}}$ is the Reynolds number at which fully rough flow commences. Determination of the transitional behaviour between these two limits requires knowledge of the boundary layer profile in the transitional regime, so that one can integrate for $\overline{U}$. Shockling *et al.* (2006) showed that in the overlap region, equation (2.3) fits the data well at all the Reynolds numbers. Since the velocity defect data show universal collapse for all the Reynolds numbers in outer-layer variables, the wake function, defined by Coles (1956), was evaluated by subtracting equation (2.3) from the experimental data. The wake function, $W(y^+)$, is shown in figure 10 plotted against $\log(y^+) - \log(D^+/2)$, where D^+ is the pipe diameter in viscous units, so that the ranges are identical for all the datasets. This function is independent of viscosity as shown by the universal collapse, for Reynolds numbers greater than 181×10^3.

To evaluate the friction factor and the Reynolds number for a given c_1 and roughness Reynolds number k_{s}^+, we need to reconstruct a velocity profile that can be integrated to evaluate $\bar{U}$. The expression for the mean velocity in terms of integration over inner variables is

$$\bar{U} = \frac{\nu 8}{D} \int_0^{D^+/2} \left(\frac{1}{2} - \frac{y^+ \nu}{D u_\tau} \right) U^+(y^+) \mathrm{d}y^+. \tag{3.1}$$

For a given roughness Reynolds number in the transitional regime, $c_2 = k_s^+$, we have an associated velocity profile shift, $c_3 = \Delta U/u_\tau$, as shown in figure 6*a*. For a specified relative roughness c_1, we have $u_\tau/\nu = c_2/(3c_1 D)$. Hence, the limit of integration of equation (3.1) is $D^+/2 = c_2/(6c_1)$ and therefore

$$Re_D = \frac{\bar{U}D}{\nu} = 8\int_0^{0.167c_2/c_1} \left(\frac{1}{2} - \frac{3c_1}{c_2}y^+\right) U^+(y^+)\mathrm{d}y^+. \tag{3.2}$$

The functional form of the full velocity profile, $U^+(y^+)$, is then a combination of the shifted (relative to smooth wall) logarithmic function and the universal wake function,

$$U^+ = f(y^+) = \frac{1}{\kappa}\ln(y^+) + B + c_3 + \Pi(\eta). \tag{3.3}$$

The span of the wake function is $\log(y^+) - \log(D^+/2) = -2$. Since the end point of the wake function is $D^+/2$, we can solve for the y^+ upper limit of the log-law region and construct $U^+(y^+)$ explicitly. Equation (3.2) is then integrated to solve for Re_D. For $y^+ < 60$, a power-law fit was made to the data of the form $U^+ = B(y^+)^\alpha$ to blend smoothly from the wall to the log law. The results for the friction factor are relatively insensitive to the nature of the near-wall fit.

Once the Reynolds number has been found, the associated friction factor can be determined from

$$\lambda = 8\frac{(u_\tau/\nu)^2}{Re_D^2} = \frac{8}{9}\frac{(c_2/c_1)^2}{Re_D^2}, \tag{3.4}$$

and the friction factor–Reynolds number relationship in transitional region for an arbitrary relative roughness, $c_1 = k_{\mathrm{rms}}/D$, can be evaluated. Calculated transitional to fully rough curves for a honed surface are shown in figure 10*b* for a number of relative roughness values. The beginning and end points of the transition are marked by open symbols. Figure 10*b* also shows the Colebrook curves for the equivalent sand-grain roughnesses. In the transitional regime, the disparities between the Colebrook curves and those calculated with the method used here are significant. Whereas honed surface roughness displays an inflectional friction factor relationship, the Colebrook curves monotonically depart from the smooth curve and approach the fully rough value from above. This technique can be applied to generate a series of curves once a single velocity shift $\Delta U/u_\tau$ versus roughness Reynolds number k_s^+ relationship has been determined. Allen *et al.* (2005) shows how this technique can be applied to the datasets of Nikuradse (1933) to produce a family of friction factor curves.

In the spirit of developing a model for the way the flow imparts shear stress, the work of Gioia & Chakraborty (2006) represents the first attempt to give a physical basis to the collection of resistance curves of Nikuradse (1933). The analysis proceeds using the energy spectrum to determine the velocity of eddies of size s as $u_s = \int_0^s E(\sigma)\sigma^{-2}\mathrm{d}\sigma$, where $E(\sigma)$ represents the energy spectrum of eddies of size σ. $E(\sigma)$ was approximated using the Kolmogorov inertial spectrum with corrections to model the dissipative and inertial range, giving

$$u_s^2 = \frac{2}{3}\kappa_{\mathrm{u}}\bar{U}^2\int_0^{s/R} x^{-1/3}c_{\mathrm{d}}\left(\frac{bRe_{\mathrm{R}}^{-3/4}}{x}\right)c_{\mathrm{e}}(x)\mathrm{d}x. \tag{3.5}$$

The functions c_{d} and c_{e} represent the dissipative and energy spectrum corrections, expressed as $c_{\mathrm{d}}(\eta/\sigma) = \exp(-\beta\eta/\sigma)$, where η is the Kolmogorov length-scale and $c_{\mathrm{e}}(\sigma/R) = (1+\gamma(\sigma/R)^2)^{-17/6}$. Using a physical argument that

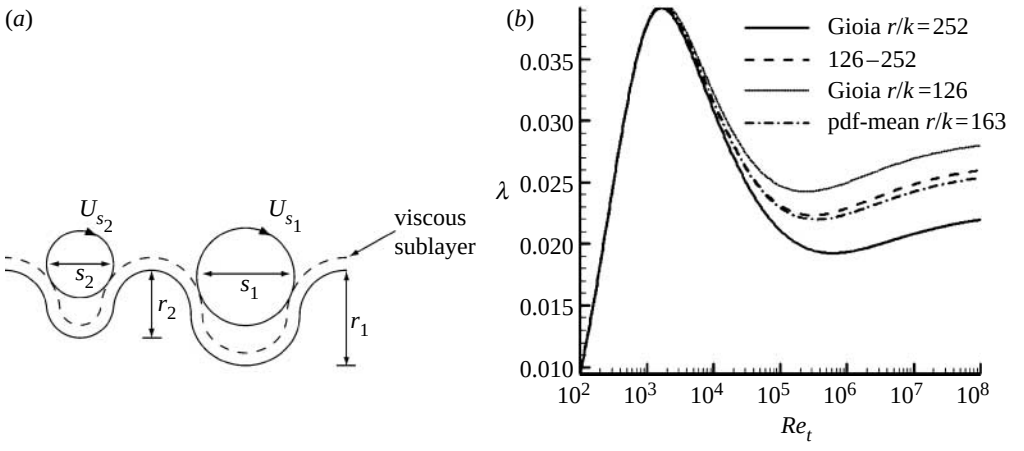

Figure 11. (*a*) Definition of roughness elements and (*b*) results from the model of Gioia & Chakraborty (2006).

relates the transfer of momentum across a roughness element of size s, Gioia & Chakraborty (2006) showed that the shear stress on the surface scales as $\tau \simeq \rho \bar{U} u_s$, which can be transformed into the friction factor as $\lambda \propto u_s/\bar{U}$. The expression for u_s was then integrated to derive an expression for λ. The resulting calculations showed the presence of an inflectional regime in the friction factor. This was explained in terms of the shear stress in this regime being dominated by eddies of a dissipative scale. The analysis of Gioia & Chakraborty (2006) deals with the shear stress imparted to a roughness element of a specific size. However, this formulation also allows for the inclusion of a probability distribution of roughness sizes, as suggested in Gioia & Bombardelli (2002), which may be more representative of natural or commercial roughness. To extend the analysis of Gioia & Chakraborty (2006), two types of multiple scale surface distributions were investigated, one bimodal and the other Gaussian. The bimodal distribution consisted of equal number of cavities of relative sizes $R/k=252$ and $R/k=126$. The shapes of the cavities are shown in figure 11*a*. The results for the associated friction factor (figure 11*b*) show a shift towards the monodisperse $R/k=126$ results, indicating a disproportionate effect from the larger cavity in determining the wall shear stress. The distribution of cavity sizes for the second simulation was Gaussian, more representative of the honed rough pipe surface, centred on a mean value of $R/k=190$. The relative roughnesses $R/k=126$ and 252 represent one standard deviation away from the mean. The results for friction factor again fall between the two monodisperse distributions. What may be significant from these preliminary calculations with representative surface distributions is that the 'depth' of the troughs in the friction factor results does not appear to be affected by the presence of multiple scales. It also appears that the incorporation of multiple scales into the model has not resulted in multiple regions of inflection. The presence of the inflection in the model of Gioia & Chakraborty (2006) appears to be invariant with respect to a variation of surface geometry. This may in turn suggest that eddies of a dissipative scale are always important in the production of shear stress over rough surfaces, provided the ratio of R/k is large.

4. Conclusions

We have used the Princeton University Superpipe, capable of generating Reynolds numbers from 31×10^3 to 35×10^6, to study the effects of a honed surface roughness on fully developed turbulent pipe flow. The Reynolds number range for the experiment was 50×10^3–30×10^6. Over this range of Reynolds number, the flow exhibits three turbulent regimes: hydraulically smooth; transitional; and fully rough. The results indicate the following.

— The friction factor behaviour of a honed surface in the transitional regime does not follow the Colebrook relationship (Colebrook & White 1937; Colebrook 1939) and instead exhibits behaviour more typical of Nikuradse's sand-grain roughness (Nikuradse 1932, 1933).
— The equivalent sand-grain roughness of the surface was found to be $k_s \simeq 3.0k_{rms}$, and the flow showed the first symptoms of roughness when $k_s^+ \approx 3.5$.
— The original Superpipe experiments were hydraulically smooth for $Re_D \leq 27\times10^6$ (as argued by Zagarola & Smits 1998 and also Wosnik *et al.* 2000).
— For all conditions of roughness, logarithmic scaling was apparent at higher Reynolds numbers with the same constants determined for smooth pipes.
— The mean velocity and turbulence intensity profiles in outer-layer scaling collapse on the same scaling as for smooth surfaces, providing strong support for Townsend's hypothesis for this particular roughness. The streamwise rough pipe spectra also agree with the previous smooth pipe data, indicating that there is no change in the structure of the turbulence in the outer region of the flow.
— The data for the size of the velocity shift $\Delta U/u_\tau$ versus k_s^+ have been used to develop a series of transitional friction factor curves for honed pipes of arbitrary relative roughness. This technique relies on the universal features of the velocity profiles, rather than an arbitrary curve fit to experimental data.
— The inflection in the transitional regime predicted by the model of Gioia & Chakraborty (2006) appears to be invariant with respect to a variation of surface geometry, which may suggest that eddies of a dissipative scale are always important in the production of shear stress over rough surfaces, provided the ratio of R/k is large.

The support of ONR under grant N00014-03-1-0320 (Ron Joslin) and NSF under grant CTS-0306691 (Michael Plesniak) is gratefully acknowledged. G.J.K. was partially funded by the Princeton University as a Council on Science and Technology Fellow.

References

Allen, J. J., Shockling, M. A. & Smits, A. J. 2005 Evaluation of a universal transition resistance diagram for pipes with honed surfaces. *Phys. Fluids* **17**, 121 702–121 706. (doi:10.1063/1.2145753)

Barenblatt, G. I. & Chorin, A. J. 1998 Scaling of the intermediate region of wall-bounded turbulence: the power law. *Phys. Fluids* **10**, 1043–1044. (doi:10.1063/1.869788)

Barenblatt, G. I., Chorin, A. J. & Prostokishin, V. M. 1997 Scaling laws for fully developed turbulent flow in pipes. *Appl. Mech. Rev.* **50**, 413–429.

Bradshaw, P. 2000 A note on 'critical roughness height' and 'transitional roughness'. *Phys. Fluids* **12**, 1611–1614. (doi:10.1063/1.870410)

Colebrook, C. F. 1939 Turbulent flow in pipes, with particular reference to the transitional region between smooth and rough wall laws. *J. Inst. Civil Eng.* **11**, 133–156.

Colebrook, C. F. & White, C. M. 1937 Experiments with fluid friction in roughened pipes. *Proc. R. Soc. A* **161**, 367–378.

Coles, D. 1956 The law of the wake in the turbulent boundary layer. *J. Fluid Mech.* **1**, 191–226. (doi:10.1017/S0022112056000135)

Flack, K. A., Schultz, M. P. & Shapiro, T. A. 2005 Experimental support for Townsend's Reynolds number similarity hypothesis on rough walls. *Phys. Fluids* **17**, 035 102. (doi:10.1063/1.1843135)

George, W. K. & Castillo, L. 1997 Zero-pressure-gradient turbulent boundary layer. *Appl. Mech. Rev.* **50**, 689–729.

Gioia, G. & Bombardelli, F. A. 2002 Scaling and similarity in rough channel flows. *Phys. Rev. Lett.* **88**, 014 501. (doi:10.1103/PhysRevLett.88.014501)

Gioia, G. & Chakraborty, P. 2006 Turbulent friction in rough pipes and the energy spectrum of the phenomenological theory. *Phys. Rev. Lett.* **96**, 044 502. (doi:10.1103/PhysRevLett.96.044502)

Krogstad, P. & Antonia, R. A. 1999 Surface roughness effects in turbulent boundary layers. *Exp. Fluids* **27**, 450–460. (doi:10.1007/s003480050370)

Kunkel, G. J. & Smits, A. J. 2006 Turbulence characteristics in high-Reynolds-number rough-wall pipe flow. AIAA Paper 2006–2884.

Ligrani, P. M. & Bradshaw, P. 1987 Spatial resolution and measurement of turbulence in the viscous sublayer using subminiature hot-wire probes. *Exp. Fluids* **5**, 407–417. (doi:10.1007/BF00264405)

MacMillan, F. A. 1956 Experiments on Pitot-tubes in shear flow. Report R&M 3028, Aero. Res. Counc.

McKeon, B. J. & Smits, A. J. 2002 Static pressure correction in high Reynolds number fully developed turbulent pipe flow. *Meas. Sci. Tech.* **13**, 1608–1614. (doi:10.1088/0957-0233/13/10/314)

McKeon, B. J., Li, J., Jiang, W., Morrison, J. F. & Smits, A. J. 2004*a* Further observations on the mean velocity distribution in fully developed pipe flow. *J. Fluid Mech.* **501**, 135–147. (doi:10.1017/S0022112003007304)

McKeon, B. J., Swanson, C. J., Zagarola, M. V., Donnelly, R. M. & Smits, A. J. 2004*b* Friction factors for smooth pipe flow. *J. Fluid Mech.* **511**, 41–44. (doi:10.1017/S0022112004009796)

McKeon, B. J., Zagarola, M. V. & Smits, A. J. 2005 A new friction factor relationship for fully developed pipe flow. *J. Fluid Mech.* **538**, 429–443. (doi:10.1017/S0022112005005501)

Moody, L. F. 1944 Friction factors for pipe flow. *Trans. ASME* **66**, 671–684.

Morrison, J. F., Jiang, W., McKeon, B. J. & Smits, A. J. 2002 Reynolds-number dependence of streamwise velocity spectra in turbulent pipe flow. *Phys. Rev. Lett.* **88**, 214 501–214 504. (doi:10.1103/PhysRevLett.88.214501)

Morrison, J. F., McKeon, J., Jiang, W. & Smits, A. J. 2004 Scaling of the streamwise velocity component in turbulent pipe flow. *J. Fluid Mech.* **508**, 99–131. (doi:10.1017/S0022112004008985)

Nikuradse, J. 1932 *VDI Forschungsheft Arb. Ing.-Wes.* **356**. In translation, *NACA TT F-10 359.*

Nikuradse, J. 1933 Laws of flow in rough pipes. *VDI Forschungsheft* **361**. In translation, *NACA TM 1292*, 1950.

Perry, A. E., Hafez, S. & Chong, M. S. 2001 A possible reinterpretation of the Princeton superpipe data. *J. Fluid Mech.* **439**, 395–401. (doi:10.1017/S0022112001004840)

Schlichting, H. 1979 *Boundary layer theory*, 7th edn. New York, NY: McGraw-Hill.

Shockling, M. A. 2005 Turbulent flow in a rough pipe. MSE dissertation, Princeton University.

Shockling, M. A., Allen, J. J. & Smits, A. J. 2006 Effects of machined surface roughness on high-Reynolds-number turbulent pipe flow. *J. Fluid Mech.* **564**, 267–285.

Townsend, A. A. 1976 *The structure of turbulent shear flow.* Cambridge, UK: Cambridge University Press.

Wosnik, M., Castillo, L. & George, W. K. 2000 A theory for turbulent pipe and channel flows. *J. Fluid Mech.* **421**, 115–145. (doi:10.1017/S0022112000001385)

Zagarola, M. V. 1996 Mean-flow scaling of turbulent pipe flow. Doctoral dissertation, Princeton University.

Zagarola, M. V. & Smits, A. J. 1998 Mean-flow scaling of turbulent pipe flow. *J. Fluid Mech.* **373**, 33–79. (doi:10.1017/S0022112098002419)